

# AngioMap is a Novel Image Analysis Algorithm for Assessment of Plasma Cell Distribution Within Bone Marrow Vascular Niche

Mohamed E. Salama, MD,\*† Holger Lange,‡ Sheryl R. Tripp, BS, MT (ASCP), QIHC (ASCP),† Jessica Kohan,† Nicholas D. Landis,‡ Joseph S. Krueger, PhD,‡ and Steven J. Potts, PhD, MBA‡

**Abstract:** The ability to characterize distribution of neoplastic hematopoietic cells and their progenitors in their native microenvironment is emerging as an important challenge and potential therapeutic target in many disease areas, including multiple myeloma. In multiple myeloma, bone marrow (BM) angiogenesis is typically increased and microvessel density is a known indicator of poor prognosis. However, the difficulty of consistently measuring 3D vessels from 2D cut sections has previously limited the study of spatial distribution of plasma cells (PC) and their interaction with BM microenvironment. The aim of the study is to report a novel method to study myeloma cells spatial distribution within their hematopoietic niche context using readily available tissue sections and standard histology approaches. We utilized a novel whole-tissue image analysis approach to identify vessels, and then applied computational grown regions extended out from each vessel at 15, 35, 55, 75, and 100  $\mu\text{m}$  to identify the spatial distribution of PC on CD34/CD138 double-stained core biopsy slides. Percent PC to total cells (TC) was significantly higher at  $< 15 \mu\text{m}$  distance compared with those at 16 to 35, 36 to 55, 56 to 75, and 76 to 100  $\mu\text{m}$  distance ( $P = 0.0001$ ). Similarly, PC/TC at  $< 35 \mu\text{m}$  region was significantly higher compared with 36 to 55 ( $P = 0.0001$ ), 56 to 75 ( $P \leq 0.0001$ ), and 76 to 100 ( $P = 0.0002$ )  $\mu\text{m}$  distances. The mean PC/TC differences in the spatial gradient of 36 to 55, 56 to 75, and 76 to 100  $\mu\text{m}$  distance regions were not significant. Our findings suggest possible preferential advantage to neoplastic PC in the proximity of blood vessels compared with other hematopoietic marrow cells. We demonstrate the feasibility of analyzing the spatial distribution of PC, and possibly other hematopoietic/stem cells in their microenvironment, as characterized by the distance to vessels in BM using a novel image analysis approach.

**Key Words:** multiple myeloma, special distribution, image analysis, bone marrow, microvessels density

(*Appl Immunohistochem Mol Morphol* 2013;00:000–000)

The increased tumor vascularization was long recognized<sup>1–3</sup>; however, the concept of tumors being angiogenesis dependent was introduced only in the last few decades.<sup>4–6</sup> Recent advances in our understanding of tumor neovascularization have emerged with several novel mechanisms of tumor neovascularization being proposed. Similar to solid tumors, the extent of bone marrow (BM) angiogenesis has been reported as a strong indicator of biological potency of malignant clone and a predictor of survival in newly diagnosed patients with multiple myeloma (MM).<sup>7–8</sup> Researchers also found highly significant correlation between microvessel density (MVD) (as a parameter of angiogenesis intensity) and histologic grade of tumor, extent of BM infiltration, proliferative activity, and predicting response to treatment in MM.<sup>7–9</sup> Although it is not currently included in MM best practice guidelines, MVD was proposed to be performed routinely on BM biopsies.<sup>7</sup>

Another important yet underappreciated factor of predicting response and anticancer drug resistance is the limited ability of drugs to penetrate tumor tissue and to reach all of the tumor cells in a potentially lethal concentration. To reach all viable cells in the tumor, anticancer drugs must be delivered efficiently through the tumor vasculature, cross the vessel wall, and traverse the tumor tissue. Therefore, it would be conceivable that a drug effect may decrease with increasing tumor cells distance from tumor blood vessels (Bl.V.) and consequently, cells at increasing distances from vessels are likely to be resistant to therapy.<sup>10</sup>

Several methods have been proposed for MVD determination including traditional hot spot techniques and computer-assisted image analysis. Few reports have proposed using spatial distribution of hematopoietic cells in BM and relevance of natural microenvironment to stem cell behavior.<sup>11,12</sup> However, methods that characterize distribution of neoplastic plasma cells (PC) in the native microenvironment of BM are lacking. In this study we report a novel image analysis technique that not only can

Received for publication February 9, 2013; accepted March 30, 2013.  
From the \*Department of Pathology, University of Utah; †ARUP Reference Lab Research Institute, Salt Lake City, UT; and ‡Flagship Biosciences, Boulder, CO.

H.L., N.D.L., J.S.K., and S.J.P., are employee of Biosciences, Boulder, CO. The remaining authors declare no conflict of interest.

Reprints: Mohamed E. Salama, MD, Department of Pathology, University of Utah, 500 Chipeta Way, Salt Lake City, UT 84108 (e-mail: mohamed.salama@path.utah.edu).

Copyright © 2013 by Lippincott Williams & Wilkins

evaluate MVD but also the spatial distribution of PC and investigate their relation to both Bl.V. as well as other normal hematopoietic cells in BM.

## METHODS

### Case Selection

A total of 31 consecutive diagnostic BM biopsies with clonal PC and adequate diagnostic materials from the files of the Department of Pathology at the University of Utah were included in the analysis. Cases with sub-optimal biopsy materials were excluded.

### Immunohistochemical Stains

Double staining for CD34 and CD138: CD34 (QBend10 clone; Ventana) and CD138 (B-A38 clone; AbD Serotec, Raleigh, NC). Slides are cut at 4  $\mu$ m on positively charged slides, allowed to air dry, and then placed at 55 to 60°C in an oven for 30 minutes. The following steps are performed on the Ventana automated immunostainer at 37°C (XT/ULTRA; Ventana Medical Systems, Tucson, AZ).

Performed on the XT instrument—deparaffinization: slides are deparaffinized with EZ Prep solution (Ventana Medical Systems). For CD34: epitope retrieval is performed using CC1 for 30 minutes; primary antibody (predilute) for 40 minutes at 37°C; blocking step (levamisole) followed by detection with the Enhanced Alkaline Phosphatase Red detection kit (Ventana Medical Systems). Slides are then removed from the XT instrument and placed on the ULTRA instrument. For CD138 (B-A38): epitope retrieval is performed using CC1 for 36 minutes at 95°C; primary antibody diluted at 1:1000 for 40 minutes at 37°C; the A/B blocking kit is applied (Ventana Medical Systems) followed by detection with the IView DAB detection kit (Ventana Medical Systems). Counterstained for 8 minutes with hematoxylin (Ventana Medical Systems) and dehydrated in graded ethanol's (70%  $\times$  1, 95%  $\times$  2, 100%  $\times$  2) 1 minute each. Cleared in 4 changes of xylene, 10 dips each followed by coverslip.

### Image Analysis

#### Enumeration of Total PC

PC% was determined on adequate CD138-stained core biopsy by whole-slide imaging as we previously described<sup>13</sup> using Aperio's Membrane IHC algorithm (Aperio Technologies, Vista, CA).

#### Evaluation of PC Distribution

CD34 (endothelial marker)/CD138 (PC marker) dual-stained (Fig. 1A) slides were digitized using the Aperio ScanScope XT slide scanner (Aperio Technologies). AngioMap, an image analysis program (Flagship Biosciences, Boulder, CO), was written in C++ for the Aperio ImageScope slide viewer and applied for evaluation of PC to vessels distance criteria. The process for image analysis is described briefly. Color deconvolution<sup>14</sup> digitally separated the CD34 (Alkaline Phosphatase Red) staining from the DAP and hematoxylin counterstain.

Endothelial cells/vessels (Fig. 1B) were identified using morphologic image analysis criteria. MVD was calculated as the number of vessels divided by the area. Regions were then automatically identified at 15, 35, 55, 75, and 100  $\mu$ m from these vascular endothelial cells.

Each distance segment was evaluated independently from other segment (ie, the 35  $\mu$ m segment is represented only by the region between 15 and 35  $\mu$ m) (Fig. 2A). The percentage of PC to total cells (TC) (TC = PC + normal hematopoietic cells) within each of the distance segments was calculated and recorded across hematopoietic areas of each slide, excluding bone and other regions in the slide with histology artifacts or poorly scanned areas (Fig. 2B).

The percent PC/TC was computed using AngioMap modified cell membrane algorithm (Fig. 3).

### Data Analysis

GraphPad Prism software was used for statistical analysis. The statistical analysis was done using paired Student *t* test. Significance of the tests was set at  $P < 0.05$ .

## RESULT

### Study Population

Samples from 31 patients (22 males and 9 females) represented study population. Patients ranged in age from 40 to 78 years old (mean 60 y). All cases had a confirmed PC dyscrasia (28 MM, 1 smoldering myeloma, and 2 monoclonal gammopathy of uncertain significance).

### Vessels Detection and MVD Analysis

The first step of analysis involved vessel density analysis performed on whole-stained section for the CD34 (Alkaline Phosphatase Red) with output parameters of MVD and vessel areas. MVD varied between cases and range from 0.3 to 108.59 vessels/mm<sup>2</sup> (mean, 22.79) and correlated with vessel area that ranges from 0.14 to 7.74 mm<sup>2</sup> (mean, 1.72).

### Spatial Distribution of PC

After identification of Bl.V., AngioMap-generated computational grown distinct regions extended out from each vessel at 15, 35, 55, 75, and 100  $\mu$ m. Membrane IHC image analysis algorithm was applied to each region for counting CD138-positive PC and CD138-negative hematopoietic cells.

Results of AngioMap analysis of PC percent (PC/TC) at regions of < 15, 16 to 35, 36 to 55, 56 to 75, and 76 to 100  $\mu$ m distance from vessels ranged from 4.72% to 99.78%,  $m = 54.90\%$ ; 1.6% to 98.98%,  $m = 45.62\%$ ; 2.29% to 98.65%,  $m = 43.21\%$ ; 1.95% to 98.88%,  $m = 41.6\%$ ; and 2.18% to 98.02%, 41.32%, respectively. In 5 cases, the PC/TC was consistently high ( $\geq 90\%$ ) throughout all analysis regions.

PC percent (PC/TC) ranged from 1.48% to 98.87% ( $m = 43.27\%$ ). On average 28% of PC (range, 9% to

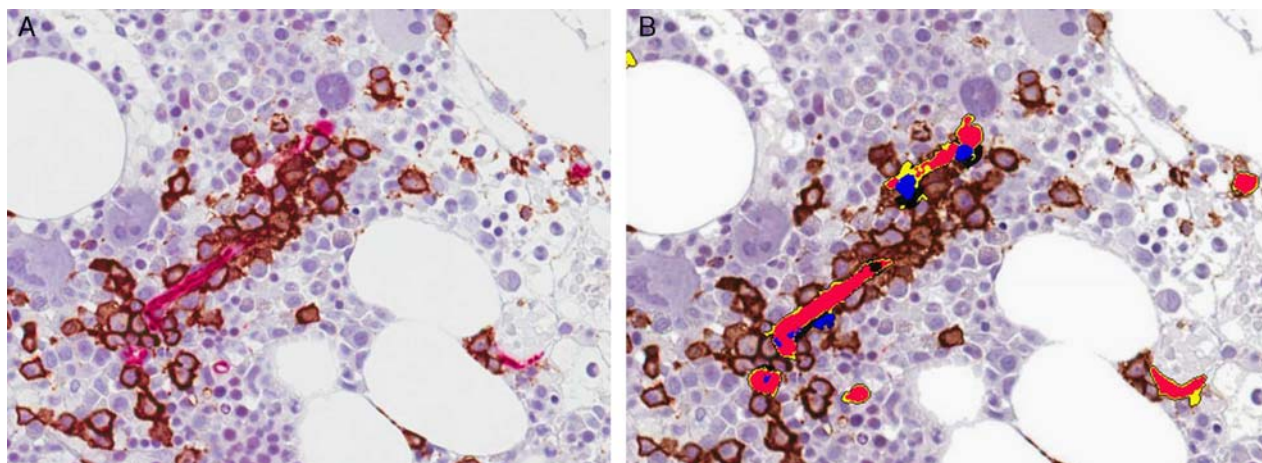


**FIGURE 1.** A, Double immunohistochemical staining for CD34 (Alkaline Phosphatase Red) and CD138 (DAP) before image analysis (original magnification,  $\times 200$ ). CD34 highlight the blood vessels and CD138 highlight plasma cells. B, A generated markup image after vessel density analysis. Vessels areas are marked in red.

60%) resided within 100  $\mu\text{m}$  of Bl.V. and 38% (average) of these (range, 20% to 58%) were within 35  $\mu\text{m}$  of Bl.V.

Percent PC/TC was significantly higher at  $< 15 \mu\text{m}$  compared with those at 16 to 35 ( $P = 0.0001$ ), 36 to 55 ( $P \leq 0.0001$ ), 56 to 75 ( $P \leq 0.0001$ ), and 76 to 100

( $P \leq 0.0001$ )  $\mu\text{m}$  distance in all cases. PC/TC at  $< 35 \mu\text{m}$  region was significantly higher compared with 36 to 55 ( $P = 0.0001$ ), 56 to 75 ( $P \leq 0.0001$ ), and 76 to 100 ( $P = 0.0002$ )  $\mu\text{m}$  distances. PC/TC was higher at 16 to 35  $\mu\text{m}$  region compared with 36 to 55 ( $P = 0.04$ ), 56 to 75

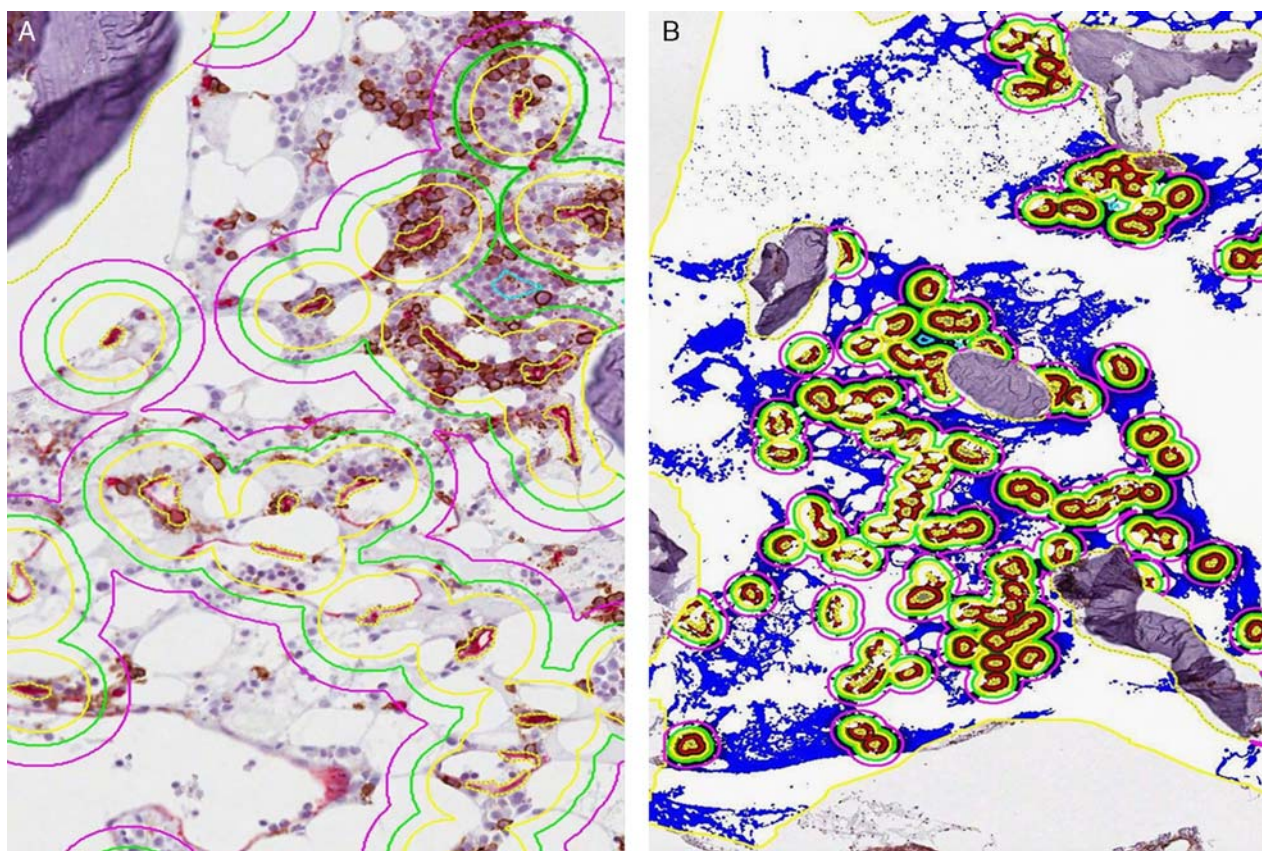


**FIGURE 2.** A, After identification of Bl.V., AngioMap-generated computational grown distinct regions extended out from each vessel at 15, 35, 55, 75, and 100  $\mu\text{m}$ . The colored yellow, green, and red lines mark 35, 55, and 75  $\mu\text{m}$  distances from vessels. B, A markup output analysis image with the grown regions applied on the whole slide excluding bone.

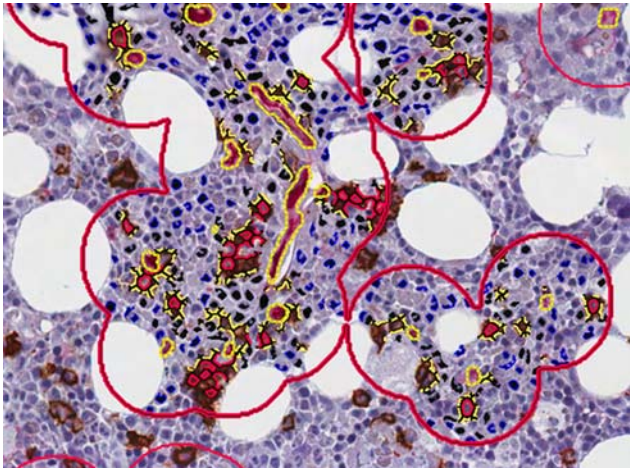


**FIGURE 3.** A high-power magnification of membrane IHC image analysis algorithm applied to 1 region segment (red line) after the vessels detection. Note the elongated vessel structures with Alkaline Phosphatase Red staining and dotted yellow outlines. The membrane IHC image analysis algorithm is subsequently applied for counting CD138-positive plasma cells (DAP-stained cells highlighted in red and yellow based on staining intensity) and CD138 negative hematopoietic cells without staining (blue nuclei).

( $P \leq 0.006$ ), and 76 to 100 ( $P = 0.014$ )  $\mu\text{m}$  distance. The largest drop of PC/TC was noted at 16 to 35  $\mu\text{m}$  distance segment from BL.V. (Fig. 4).

There was a mean of difference of 11.69% and 6.29% of PC/TC over at distances of  $< 15 \mu\text{m}$ , and  $< 35 \mu\text{m}$  when compared with those of  $> 35 \mu\text{m}$  from the vascular structure, respectively ( $P \leq 0.0001$ ). We further

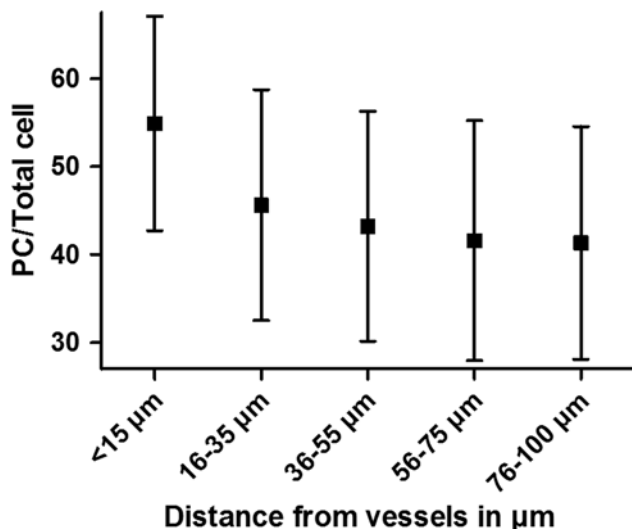


**FIGURE 4.** The graph shows a plot of PC/TC means (boxes) in each of the regions segments based on distance from blood vessels. Distance from blood vessels is plotted on the x axis in  $\mu\text{m}$ . Error bars represent 95% CI. CI indicates confidence interval; PC, plasma cells; TC, total cells.

note that the mean PC/TC differences in the spatial gradient of 36 to 55, 56 to 75, and 76 to 100  $\mu\text{m}$  distance regions were not significant at 1.6% ( $P = 0.0837$ ) and 0.27% ( $P = 0.797$ ), respectively.

## DISCUSSION

The predictive value of MVD and angiogenesis in MM as well other tumors is well established.<sup>7,15</sup> However, few studies investigated the spatial patterning of tumor cells around BL.V.; a major component of the tumor microenvironment.<sup>16,17</sup> The spatial distribution of PC and density gradient around BL.V. is an unexplored area of investigation with the potential of further expanding our knowledge of tumor behavior and biology. In this study we report a novel developed method that allows analyzing neoplastic PC in their BM vascular niche context using readily available tissue sections and standard histology approaches.

Our results revealed a statistically significant increase of PC/TC ratio in the proximity of BL.V. at  $> 15$  and 16 to 35  $\mu\text{m}$  regions compared with further distances. There was also a mean of difference of 11.69% and 6.29% of PC/TC over at distances of  $< 15 \mu\text{m}$ , and  $< 35 \mu\text{m}$  when compared with those of  $> 35 \mu\text{m}$  from the vascular structure, respectively ( $P \leq 0.0001$ ). We further note that the mean PC/TC differences between the spatial gradient of regions of 36 to 55, 56 to 75, and 76 to 100  $\mu\text{m}$  distance were not significant. These findings suggest a survival advantage to neoplastic PC in the proximity of BL.V. compared with other hematopoietic marrow cells.

The drop in the PC concentration in the 16 to 35  $\mu\text{m}$  segments is intriguing. Although the definitive mechanism of the neoplastic PC preferential localization within 35  $\mu\text{m}$  region is not fully understood, it seems intuitive that this reflects a function of mediated angiogenesis and its relation to tumorigenesis. One may speculate that the special distribution of PC in MM is the outcome of neoangiogenesis sprout formation with causing or resultant tumor cells patterning around BL.V. The process of tumor cell patterning is likely multifactorial and represents the result of a complex and temporal orchestration of multiple mechanisms involving angiogenic cytokine expression, receptor signaling states, and cell types as well as, extracellular matrix proteolysis, among other possibilities.<sup>16</sup> Plausible example is vascular endothelial growth factor (VEGF), an important mediator of vascular patterning.<sup>17</sup>

Previous studies suggested that VEGF diffusion and gradient in tissue along with metalloproteinases play a critical role in the pathologic condition through matrix-sequestered VEGF and modulating angiogenesis. Vempati and colleagues used a 3D molecular-detailed reaction-diffusion model of VEGF ligand-receptor kinetics and transport to test models of VEGF transport and degradation in the extracellular environment surrounding and endothelial sprout. In their study, they highlighted possible mechanisms by which information in the VEGF distribution and degradation can be used to guide vascular patterning and explain vascular branching complexity and

the regulation of angiogenesis and tumor growth by proteases. Sophisticated cell-based modeling and simulation studies are required to interrogate potential factors involved in tumor cells and vascular patterning.

Another important reason for characterization of spatial distribution of tumor cells around Bl.V. is its potential relevance to the ability of the anticancer drug to cross vessels, penetrate tumor tissue, and reach all tumor cells in a lethal concentration. The tumor microenvironment is relevant not only for the gradient in drug concentration but also to gradients in rate of cell proliferation and by regions of hypoxia. Interestingly, previous studies reported gradient of oxygen concentration and drop of pH in relation to the distance from nearest Bl.V. in solid tumor with the highest drop at 20 to 40  $\mu\text{m}$  and hypoxia at 70  $\mu\text{m}$ .<sup>10,16</sup>

In conclusion, we report herein a novel method for characterization of PC spatial distribution around Bl.V. in BM. Although the methodology of this study focuses on MVD and characterization of spatial distribution of PC within a given distance of blood supply, it can be applied also to the bone surface. In addition, this methodology approach can be generalized to any type of tumor cells, stem cells, or other cells of interest and the principle can be easily applied to other neoplastic hematopoietic or stem cells. The findings of significantly increased PC concentration in the proximity of Bl.V. at >35  $\mu\text{m}$  regions compared with further distances in this study, strongly support the commonly accepted ideas of vascular niche dependence of PC dyscrasias and the prognostic predictive role of MVD.

## REFERENCES

- Goldman E. The growth of malignant disease in man and the lower animals with special reference to the vascular system. *Proc R Soc Med.* 1908;1:1–13.
- Lewis W. The vascular pattern of tumors. *Johns Hopkins Hosp Bull.* 1927;41:156–162.
- Fox SB, Harris AL. Histological quantitation of tumour angiogenesis. *APMIS.* 2004;112:413–430.
- Weidner N, Folkman J, Pozza F, et al. Tumor angiogenesis: a new significant and independent prognostic indicator in early-stage breast carcinoma. *J Natl Cancer Inst.* 1992;84:1875–1887.
- Weidner N, Semple JP, Welch WR, et al. Tumor angiogenesis and metastasis—correlation in invasive breast carcinoma. *N Engl J Med.* 1991;324:1–8.
- Horak ER, Leek R, Klenk N, et al. Angiogenesis, assessed by platelet/endothelial cell adhesion molecule antibodies, as indicator of node metastases and survival in breast cancer. *Lancet.* 1992;340:1120–1124.
- Bhatti SS, Kumar L, Dinda AK, et al. Prognostic value of bone marrow angiogenesis in multiple myeloma: use of light microscopy as well as computerized image analyzer in the assessment of microvessel density and total vascular area in multiple myeloma and its correlation with various clinical, histological, and laboratory parameters. *Am J Hematol.* 2006;81:649–656.
- Marisavljevic D, Markovic O, Cemerikic V, et al. Clinical and histopathological study of angiogenesis in multiple myeloma. *J Buon.* 2011;16:98–103.
- Markovic O, Marisavljevic D, Cemerikic V, et al. Expression of VEGF and microvessel density in patients with multiple myeloma: clinical and prognostic significance. *Med Oncol.* 2008;25:451–457.
- Tredan O, Galmarini CM, Patel K, et al. Drug resistance and the solid tumor microenvironment. *J Natl Cancer Inst.* 2007;99:1441–1454.
- Grassinger J, Haylock DN, Williams B, et al. Phenotypically identical hemopoietic stem cells isolated from different regions of bone marrow have different biologic potential. *Blood.* 2010;116:3185–3196.
- Grassinger J, Nilsson SK. Methods to analyze the homing efficiency and spatial distribution of hematopoietic stem and progenitor cells and their relationship to the bone marrow endosteum and vascular endothelium. *Methods Mol Biol.* 2011;750:197–214.
- Shetty S, Siady M, Mallempati KC, et al. Utility of a column-free cell sorting system for separation of plasma cells in multiple myeloma FISH testing in clinical laboratories. *Int J Hematol.* 2012;95:274–281.
- Ruifrok AC, Johnston DA. Quantification of histochemical staining by color deconvolution. *Anal Quant Cytol Histol.* 2001;23:291–299.
- Folkman J. What is the evidence that tumors are angiogenesis dependent? *J Natl Cancer Inst.* 1990;82:4–6.
- Vaupel P. Tumor microenvironmental physiology and its implications for radiation oncology. *Semin Radiat Oncol.* 2004;14:198–206.
- Vempati P, Popel AS, Mac Gabhann F. Formation of VEGF isoform-specific spatial distributions governing angiogenesis: computational analysis. *BMC Syst Biol.* 2011;5:59–83.